https://doi.org/10.5194/hess-2021-254
Preprint. Discussion started: 21 May 2021
© Author(s) 2021. CC BY 4.0 License.

Hydrology and Earth System Sciences
Discussions

Preferential Pathways for Fluid and Solutes in Heterogeneous Groundwater Systems: Self-Organization, Entropy, Work

1) Erwin Zehe, 1) Ralf Loritz, 2) Yaniv Edery, 3) Brian Berkowitz

1) Karlsruhe Institute of Technology (KIT), Institute of Water and River Basin Management, Karlsruhe, Germany; 2) Technion Israel Insstitute of Technology, Haifa, Israel; 3) Department of Earth and Planetary Sciences, Weizmann Institute of Science, Rehovot, Israel

Corresponding author: Erwin Zehe (Erwin.Zehe@kit.edu)

Abstract

Patterns of distinct preferential pathways for fluid flow and solute transport are ubiquitous in heterogeneous, saturated and partially saturated porous media. Yet, the underlying reasons for their emergence, and their characterization and quantification, remain enigmatic. Here we analyze simulations of steady state fluid flow and solute transport in two-dimensional, heterogeneous saturated porous media with a relatively short correlation length. We demonstrate that the downstream concentration of solutes in preferential pathways implies a downstream declining entropy in the transverse distribution of solute transport pathways. This reflects the associated formation and downstream steepening of a concentration gradient transversal to the main flow direction. With an increasing variance of the hydraulic conductivity field, stronger transversal concentration gradients emerge, which is reflected in an even smaller entropy of the transversal distribution of transport pathways. By defining "self-organization" through a reduction in entropy (compared to its maximum), our findings suggest that a higher variance and thus randomness of the hydraulic conductivity coincides with stronger macroscale self-organization of transport pathways. While this finding appears at first sight striking, it can be explained by recognizing that emergence of spatial self-organization requires, in light of the second law of thermodynamics, that work be performed to establish transversal concentration gradients. The emergence of steeper concentration gradients requires that even more work be performed, with an even higher energy input into an open system. Consistently, we find that the energy input necessary to sustain steady-state fluid flow and tracer transport grows with the variance of the hydraulic conductivity field as well. Solute particles prefer to move through pathways of very high power, and these pathways pass through bottlenecks of low hydraulic conductivity. This is because power depends on the squared spatial head gradient, which is in these simulations largest in regions of low hydraulic conductivity.

https://doi.org/10.5194/hess-2021-254
Preprint. Discussion started: 21 May 2021
© Author(s) 2021. CC BY 4.0 License.

Hydrology and Earth System Sciences
Discussions

1 Introduction

1.1 Preferential flow phenomena – fast, furious and enigmatic

Distinct patterns of preferential movement of water, dissolved and suspended matter are ubiquitous in fully-saturated aquifer systems (e.g., LaBolle and Fogg, 2001; Bianchi et al., 2011; Berkowitz et al., 2006), partially saturated soils (e.g., Beven and Germann, 1982) and at the land surface (e.g., Uhlenbrook, 2006). Preferential flow and solute transport in porous media commonly leads to fast, localized early arrivals and/or long tailing in temporal breakthrough curves (e.g., Berkowitz et al., 2006) and pronounced fingerprints in concentration patterns in soils (Flury et al., 1994).

Preferential flow and transport often occur along connected highly conductive networks. Some networks are formed by previous physical/chemical work performed by the fluid, as in the cases of surface rill and river networks (Howard, 1990), subsurface pipe networks (Jackisch et al., 2017), karst conduits (Groves and Howard, 1994), and fractured rock formations (Becker and Shapiro, 2000; Berkowitz, 2002). Other networks are created by soil fauna and flora as earth worm burrows (Zehe and Flühler, 2001; van Schaik et al., 2014) and plant roots (Wienhöfer et al., 2009; Tietjen et al., 2009). Although it might appear unsurprising that flow and transport through these networks dominates system behavior, effective ways to model flow and transport in these networks have been debated for more than 30 years (Beven and Germann, 1981; Šimůnek et al., 2003; Klaus and Zehe, 2011; Wienhöfer and Zehe, 2014; Berkowitz et al., 2006, Sternagel et al., 2019, 2020). Preferential flow and transport occurs, however, also in porous media without such “well-defined” networks, e.g., in coarse-grained soils due to fingering and wetting front instabilities (Blume et al., 2009; Dekker and Ritsema, 2000; Ritsema et al., 1998) and particularly in stochastically heterogeneous saturated porous media (Bianchi et al., 2011; Edery et al. 2014).

The emergence of preferential pathways in systems without well-defined networks – and their characterization – remains even more enigmatic. The numerical study of Edery et al. (2014), for example, revealed that a higher variance in the hydraulic conductivity (K) field coincided with a stronger concentration of solutes within a smaller number of preferential flow paths. If the emergence of preferential flow is indeed manifested self-organization, as argued by Berkowitz and Zehe (2020), this key finding of Edery et al. (2014) suggests that macroscale steady states of stronger organization (or higher order) emerge and persist despite a greater

https://doi.org/10.5194/hess-2021-254
Preprint. Discussion started: 21 May 2021
© Author(s) 2021. CC BY 4.0 License.

Hydrology and Earth System Sciences
Discussions

degree of subscale randomness. The related key questions we address here are (i) how spatial organization in preferential fluid flow and solute transport can be quantified, and (ii) why a larger subscale randomness might favor stronger macroscale organization.

1.2 Attempts to characterize and predict preferential transport in groundwater

The emergence of preferential pathways of fluid flow and solute transport in saturated porous media has been explored in numerous simulation studies in heterogeneous conductivity fields, to relate the spatial correlation structures of the hydraulic conductivity and velocity fields to features of anomalous transport behavior (e.g., Cirpka and Kitanidis, 2000; Willmann et al., 2008; Berkowitz and Scher, 2010; de Dreuzy et al., 2012; Morvillo et al., 2021). While velocity correlation parameters have been successfully related to statistical moments of hydraulic conductivity, it remains challenging or even impossible to a priori delineate preferential pathways exclusively based on multivariate and topological characteristics of the hydraulic conductivity field. Cirpka and Kitanidis (2000) and Willmann et al. (2008) report, for instance, the emergence of preferential pathways in the distributions of tracer travel velocities and shapes of solute plumes. These pathways were not apparent, however, from the analysis of the stationary conductivity fields. Moreover, Edery et al. (2014) demonstrate that critical path analysis (based on percolation theory), for example, does not determine the actual preferential pathways in a system; the authors suggest that the operational preferential pathways become fully apparent only when solving for fluid flow and solute transport through the domain.

Bianchi et al. (2011) explored the link between connectivity and the emergence of preferential flow paths at the MADE site, using three-dimensional, conditional, geostatistical realizations of the hydraulic conductivity field. Their simulations of flow and transport under permeameter-like boundary revealed that the first 5% of particles, arriving at the downstream domain outlet, moved through preferential flow paths carrying 40% of the flow. Fiori and Jankovic (2012) reported similar findings and stressed the rather small probability that solute particles visit highly conductive blocks particularly in case of a high variance in K. Bianchi et al. (2011) highlighted that the fraction of particle paths passing the high-conductivity regions was between 43% and 69%, while the most rapid transport passed through low-conductivity bottle necks. This is in line with the findings of Edery et al. (2014), who concluded that connectivity of rapid preferential pathways need not require connected zones of continuously high hydraulic conductivity. Along a different avenue, Bianchi and Pedretti (2017) characterized spatial

https://doi.org/10.5194/hess-2021-254
Preprint. Discussion started: 21 May 2021
© Author(s) 2021. CC BY 4.0 License.

Hydrology and Earth System Sciences
Discussions

disorder in two-dimensional conductivity fields by means of the Shannon entropy (Shannon, 1948) and related this to moments of solute breakthrough curves. Dispersion in travel times and the probability of solutes to pass through low conductivity regions were found to increase with lower order expressed by a higher geological entropy.

1.3 Preferential flow, self-organization, entropy, work – where is the connection?

The results of the studies mentioned above all underpin that (a) preferential flow and transport in heterogeneous, saturated porous media remains a largely enigmatic and emergent phenomenon, and (b) efforts to represent this behavior by means of effective transfer functions, inferred from volume-averaging based scaling of the hydraulic conductivity field, appear virtually impossible. This is why, we propose to shift the attention from the question of "where" preferential pathways emerge, to questions regarding their "macroscale organization and strength", and "the necessary physical work" to establish their self-organized emergence.

Haken (1983) defined self-organization as the emergence of ordered macroscale states, or the dynamic behavior of an open system far from thermodynamic equilibrium (TE), that arises from a synergetic interplay of microscale, irreversible processes. An ordered state is characterized by the deviation of its entropy from the entropy maximum at TE (Kondepudi and Prigogine, 1998, see section 3). This reduction in entropy, and any additional entropy produced by the internal irreversible processes, must be exported from the open system to establish order. This in turn requires physical work, and thus an input of free energy into the system, that is large enough to create and maintain the self-organized state. A classical example to illustrate that self-organization in open systems requires free energy and work, which inspired also Haken's theory of "synergetics", is a gas laser. Laser light results from coherent stimulated light emissions from all molecules in the system. Stimulated emission emerges when the energy input to the gas laser becomes sufficiently large that the number of stimulated molecules exceeds the number of molecules in the basic state. This "energetic pumping" establishes a state very far from thermodynamic equilibrium, corresponding to an even apparently negative absolute temperature in Boltzmann statistics, at which coherent emission from all individual emissions emerges. Haken (1983) postulated that a higher-order, non-local "enslavement principle" forces the individual molecules into a coherent and thus ordered behavior. This example of a critical pumping rate to establish organization of laser light will be shown below (section 4) to be analogous to fluid flow through porous media.

https://doi.org/10.5194/hess-2021-254
Preprint. Discussion started: 21 May 2021
© Author(s) 2021. CC BY 4.0 License.

Hydrology and Earth System Sciences
Discussions
Open Access
EGU

Several researchers have suggested that self-organization and the formation of complex organisms and patterns in biological and environmental systems are governed by non-local/global energetic extremal principles, in analogy to the Haken (1983) enslavement principle. Pioneering studies in this context proposed that species maximize their energy throughput (i.e., power) during evolution (Lotka, 1922 a &b) or showed that steady-state planetary heat transport may be modeled successfully with a very simple two-box model, when assuming that this state maximizes entropy production (Paltridge, 1979). This work motivated several studies that explored the possibility that energetically optimized model setups allow hydrological prediction of the land surface energy balance and evaporation (Kleidon et al., 2014; Zehe et al., 2013), rainfall runoff behavior (Zehe et al., 2013) and groundwater flow and spring discharge (Hergarten et al., 2014). These and other studies generally showed that preferential flow in connected networks allows for a more energy efficient throughput of water and matter through the system. This is because they reduce flow-weighted dissipative losses due to an increased hydraulic radius in the rill or river network compared to sheet overland flow (Howard, 1990; Kleidon et al., 2013) or in subsurface connected preferential pathways compared to matrix flow (Hergarten et al., 2014; Zehe et al., 2010).

While the second law of thermodynamic refers to physical entropy (introduced by Clausius (1857), section 3.1), information entropy (introduced by Shannon (1948)) is closely related and well suited for diagnosing spatial organization (section 3.3). The concepts of information and Shannon entropy having been used widely to characterize irreversible mixing and reaction processes and their predictability (Chiogna and Rolle, 2017), the emergence of order in distributed time series (Malicke et al., 2020), information in multiscale permeability data (Dell`Oca et al., 2020) and the role of spatial variability of rainfall and topography in distributed hydrological modelling (Loritz et al., 2018, 2021). Woodbury and Ulrych (1993) and Kitanidis (1994) used the Shannon entropy to describe the spatial-time development and dilution of tracer plumes in groundwater systems. Chiogna and Rolle (2017) expanded the dilution index for the case of reactive solute mixing in groundwater and found a critical value that indicated the complete consumption of a reactant, which was independent of advection and dispersion. Bianchi and Pedretti (2017) used the Shannon entropy to quantify spatial disorder in stochastically generated alluvial aquifers and explored its relation to the first three moments of simulated tracer break through curves. They found the average breakthrough time and its

https://doi.org/10.5194/hess-2021-254
Preprint. Discussion started: 21 May 2021
© Author(s) 2021. CC BY 4.0 License.

Hydrology and Earth System Sciences
Discussions

variance to increase with increasing geological entropy, while the skewness in travel times declined with increasing geological entropy increasing disorder.

1.4 Objectives

We thus suggest that the concepts of entropy, free energy and work hold the key to better understand why preferential flow and transport in unstructured heterogeneous, saturated porous media actually emerge. To this end, we analyze simulations of fluid flow and solute transport through stochastically heterogeneous aquifers with different degrees of randomness (variance in hydraulic conductivity), based on the results and insights of Edery et al. (2014). Specifically, we show that macroscale self-organization due to the emergence of preferential solute transport can be quantified based on the downstream decline of the Shannon entropy of the transversal concentration pattern. We also find that preferential patterns of higher order, expressed through lower entropies, emerge in case of larger variances of hydraulic conductivity. What appears almost as a paradox at first sight – in the sense that a higher subscale randomness of the medium causes a stronger spatial organization – can be explained by the fact that the power required to maintain the driving head difference in steady state increases with increasing variance of the hydraulic conductivity field. Due to this higher energy input, the fluid and solutes may perform the necessary work to form preferential transport pathways that pass rapidly through low conductivity bottlenecks and form preferential flow paths by steepening transversal concentration gradients. We show, finally, that the entropy in the corresponding breakthrough curve (BTC) increases with the variance of the hydraulic conductivity. This can be explained by recognizing that entropy cannot be consumed, due to the second law of thermodynamics. Hence, the downstream declining entropy in the transversal distribution of solute needs to be exported from the system, and this export is reflected in the higher entropy of the corresponding BTC.

2 Underlying simulations of fluid flow and transport

2.1 Media generation and numerical simulations of fluid flow

Here, we partially revisit and expand upon the numerical simulations of Edery et al. (2014), which were employed to provide insight on fluid flow and anomalous solute transport behavior. Edery et al. (2014) considered steady-state fluid flow within a two-dimensional, stochastic heterogeneous system. The flow domain measured 300 by 120 space units as discretized into

https://doi.org/10.5194/hess-2021-254
Preprint. Discussion started: 21 May 2021
© Author(s) 2021. CC BY 4.0 License.

Hydrology and Earth System Sciences
Discussions

grid cells of uniform size $\Delta x = 0.2$, $\Delta y = 0.2$, while all quantities are expressed using the same space-time units. We consider a deterministic head difference of 100, from the left (vertical) upstream boundary to the right downstream boundary; no-flow conditions are assigned to the two horizontal domain boundaries.

We generated random realizations of statistically homogeneous, isotropic Gaussian fields for the natural logarithm of the hydraulic conductivity $\ln(K)$, with exponential covariance and mean $\ln(K) = 0$, using the sequential Gaussian simulator GCOSIM3D (Gómez-Hernánez et al,. 1997). Edery et al. (2014) considered fields associated with a unit correlation length, $l = 1$, exploring the impact of different values of the variance of $\ln(K)$, i.e., $1 < \sigma^2 < 5$, on the emergence of preferential solute transport.

Figure 1a shows a realization for $\sigma^2 = 3$, corresponding to mild and strong randomness for distances larger than $3l$. The deterministic flow problem for each realization was solved using a code that is based on finite elements with Galerkin weighting functions (Guadagnini and Neuman, 1999). The corresponding hydraulic head values throughout the domain were converted to local velocities, and thus streamlines (Fig. 1b), which were in turn used for transport simulations using particle tracking. For the system considered here, we used a porosity of 0.3 (e.g., Levy and Berkowitz, 2003).

2.2 Simulated solute transport with particle tracking

Solute movement in each domain realization was simulated using the calculated streamlines, with a standard Lagrangian particle tracking method. For all domains, values of Δ and l were chosen such that $l/\Delta = 5$, to enable capture of small-scale fluctuations and advective transport features (Ababou et al., 1989; Riva et al., 2009). Along the left upstream boundary, particles are injected, by flux-weighting, and advance by advection and diffusion. The Langevin equation defines the particle displacement vector $\mathbf{r}$, starting from given particle locations at time t_k:

$$\mathbf{r} = \boldsymbol{v}[\mathbf{x}(t_k)]\delta t + \boldsymbol{d}_o \quad \text{(Eq. 1)}$$

where $\boldsymbol{v}$ is the fluid velocity vector, δt is the time step magnitude, and $\boldsymbol{d}_o$ denotes the diffusive displacement, with a modulus of $\boldsymbol{d}_o$ given by $\xi\sqrt{2D_{\mathrm{mol}}\delta t}$; ξ is a random number drawn the from

https://doi.org/10.5194/hess-2021-254
Preprint. Discussion started: 21 May 2021
© Author(s) 2021. CC BY 4.0 License.

Hydrology and Earth System Sciences
Discussions
Open Access
EGU

standard normal distribution $N[0, 1]$. A representative molecular diffusion coefficient of $D_{mol} = 10^{-9}$ m^2 s^{-1} was prescribed (Domenico and Schwartz, 1990). The advective displacements in Equation 1 are computed using the local velocities at **x** with a fixed, uniform spatial step δs. In Equation 1, the time step δt is given by $\delta t = \delta s/v$, where v is the modulus of $\boldsymbol{v}$. Reflection conditions are prescribed along the two horizontal no-flow boundaries to avoid particle leakage. As in Edery et al. (2014), we used 10^5 particles, with $\delta s = \Delta/10$.

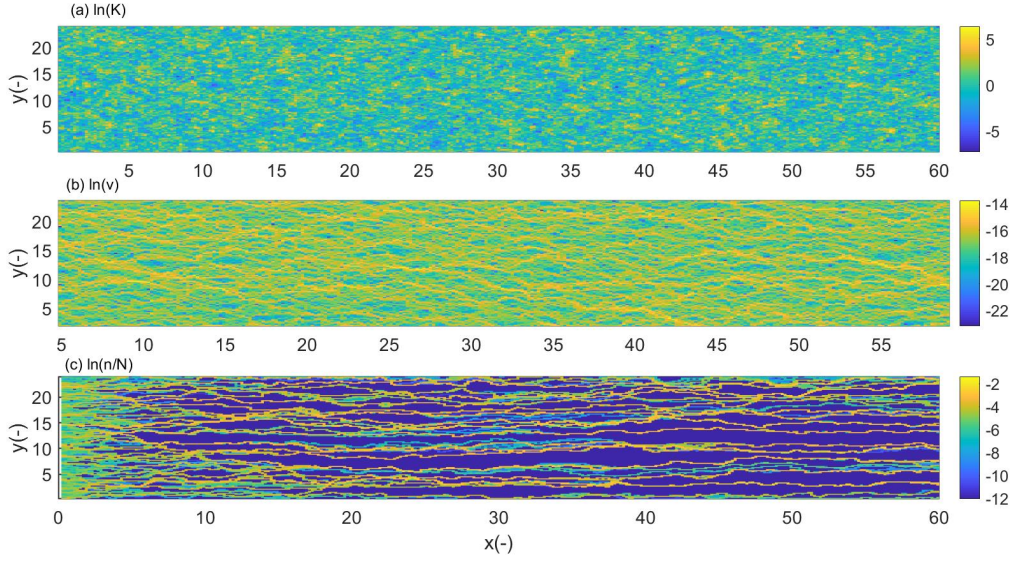

Figure 1: Examples of (a) ln(K), (b) ln(v), and (c) the cumulative number of particles that visited a grid cell in the simulation domain, normalized with the total number of particles N, on a logarithmic scale. The variance of ln(K) is $\sigma^2 = 3$.

3 Free energy, entropy and work

3.1 Thermodynamics in a nutshell: the first and the second law

We start very generally with the first law of thermodynamics, which relates the variation in internal energy U (J = kg m^2 s^{-2}) of a system to a variation of work E_{free} (J) and a variation of heat Q_h (J), while overall energy is conserved:

$$\delta U = \delta E_{free} + \delta Q_h \ (Eq. 2)$$

https://doi.org/10.5194/hess-2021-254
Preprint. Discussion started: 21 May 2021
© Author(s) 2021. CC BY 4.0 License.

Hydrology and Earth System Sciences
Discussions

Note that the capacity of a system to perform work is equivalent to "free energy", while a variation in heat is equal to the product of a variation of physical entropy S (J K^{-1}) and the absolute temperature T (K): $\delta Q_h = T\ \delta S$ as introduced by Clausius (1857). The second law of thermodynamics states that entropy is produced during irreversible processes, while it cannot be consumed. The second law implies that isolated systems, which neither exchange mass, nor energy, nor entropy with their environment, reach a dead state of maximum entropy called thermodynamic equilibrium in which all gradients have been depleted. Kleidon (2016) distinguishes three types of physical entropy: thermal entropy produced by friction and depletion of temperature gradients, molar entropy produced by mixing and depletion of chemical potential/concentration gradients, and radiation entropy produced by radiative cooling and depletion of radiation temperature differences.

From Eq. 2 and the second law, we can conclude that free energy is not a conserved property, as it corresponds to the variation in internal energy minus the variation in heat, during which entropy is produced. Free energy dissipation and entropy production are thus inseparable, and maximization of the entropy of an isolated system occurs due to conservation of energy at the expense of minimizing its free energy. An open system may nevertheless persist in steady states of lower entropy, if it is exposed to a sufficient influx of free energy to sustain the necessary physical work that needs to be performed to act against the natural depletion of the internal gradients, or even to steepen them and further reduce the entropy (as discussed for the gas laser). Order in an open system thus manifests through persistent gradients and an entropy lower than the maximum. Steps to higher order and lower entropies imply a steepening of internal gradients. This is exactly what occurs when preferential transport of solutes emerges in our transport simulations: solute particles tend to concentrate in localized pathways, thereby forming a transversal concentration gradient (according to the domain geometry shown in Fig. 1). The Shannon entropy (Shannon, 1948) is ideally suited to quantify the related entropy reduction, as detailed in section 3.3.

3.2 The free energy balance of saturated porous media

To determine the work that is performed by the fluid when flowing through heterogeneous media, we derive the free energy balance of the fluid by relating changes in hydraulic head and fluid flux to their energetic counterparts. The local formulation of the free energy balance of a groundwater system, seen as an open thermodynamic system, is determined by the

https://doi.org/10.5194/hess-2021-254
Preprint. Discussion started: 21 May 2021
© Author(s) 2021. CC BY 4.0 License.

Hydrology and Earth System Sciences
Discussions

difference/divergence of the free energy fluxes $\boldsymbol{J}^{E}_{free}$ (J s^{-1} m^{-2}) per unit area and the amount of dissipated energy per volume D (J s^{-1} m^{-3}):

$$\frac{de_{free}}{dt} = -\nabla \cdot \boldsymbol{J}^{E}_{free} - D \quad \text{(Eq. 3)}$$

where e_{free} (J s^{-1} m^{-3}) is the volumetric free energy density. Advective fluxes of relevant free energy forms are generally determined by multiplying the Darcy flux with the corresponding form of energy per unit volume. Here we account for advection of mechanical energy $\boldsymbol{J}^{E}_{H}$ (named power hereafter), gravitational potential energy $\boldsymbol{J}^{E}_{pot}$, and kinetic energy of the flowing fluid $\boldsymbol{J}^{E}_{kin}$. As energy is additive, the term $\boldsymbol{J}^{E}_{free}$ corresponds hence to the sum of the following free energy fluxes:

$$\boldsymbol{J}^{E}_{H} = \boldsymbol{q}\rho g H$$
$$\boldsymbol{J}^{E}_{pot} = \boldsymbol{q}\rho g z \quad (Eq. 4)$$
$$\boldsymbol{J}^{E}_{kin} = \boldsymbol{q}\frac{1}{2}\rho v^2$$

where ρ (kg m^{-3}) is the density of water, g (m s^{-2}) the gravitational acceleration, $\boldsymbol{q}$ (m s^{-1}) the Darcy flux, v (m s^{-1}) the absolute value of the fluid velocity, H (m) the pressure head, and z (m) the geodetic elevation. Note that while kinetic energy is proportional to v^2, the kinetic energy flux corresponds to the product of the volumetric water flux $\boldsymbol{q}$ and its kinetic energy density ½ ρv^2. Thus, kinetic energy is in fact proportional to v^3 and is usually very small. By inserting Eq. 4 into Eq. 3, we obtain:

$$\frac{de_{free}}{dt} = -\rho g \nabla[\boldsymbol{q}(H+z)] - \frac{1}{2}\rho \nabla[\boldsymbol{q}v^2] - D \quad (Eq. 5)$$

The left hand side of Eq. 5 corresponds to the change in Gibbs free energy of a fluid volume under isothermal conditions (Bolt and Frissel, 1960). This change in free energy storage on the left hand side can be decomposed into the sum of three terms as well (Zehe et al., 2019): (i) the change in storage of gravitational potential energy reflecting soil water storage changes in partially saturated soils or density changes in groundwater; (ii) the change in storage of mechanical energy reflecting changes in pressure head in groundwater or changing matric potentials in partially saturated soils; and (iii) the change in kinetic energy stored in the system, due to acceleration of the fluid. The latter is usually very small and can be neglected.

https://doi.org/10.5194/hess-2021-254
Preprint. Discussion started: 21 May 2021
© Author(s) 2021. CC BY 4.0 License.

Hydrology and Earth System Sciences
Discussions

In the case of steady-state groundwater flow, the variables H, z, ρ and v are constant in time, so that the change in free energy storage at the left hand side of Eq. 5 is zero. As we assume z to be constant along the system and neglect density changes of the fluid, the divergence in the flux of gravitational potential energy at the right hand side is zero, as well. The system under investigation hence receives solely steady-state inflow of high mechanical energy, corresponding to the upstream inflow of water at a high pressure head, and it exports water at a much lower mechanical energy at the lower downstream pressure head. The corresponding energy difference is partly dissipated and partly converted into kinetic energy of flowing fluid and dissolved solute masses. The latter is, however, usually neglected, as dissolved solute mass is much smaller. As steady-state fluid flow further implies that the divergence of $\boldsymbol{q}$ is zero as well, the free energy (Eq. 4) becomes hence:

$$\rho g \boldsymbol{q} \cdot \nabla H = -\rho v \boldsymbol{q} \cdot \nabla v - D \ (Eq. 6).$$

The left hand side is the available power per unit volume P (J s^{-1} m^{-3}) in the groundwater flux, which is partly converted into a spatial change in kinetic energy of the fluid and partly dissipated. In contrast to overland flow systems (Loritz et al., 2019; Schroers et al., 2021), the change in kinetic energy can be neglected for groundwater as it is proportional to the cube of the fluid velocity (as noted before Eq. 5). In fact, the use of Darcy's law implies that kinetic energy can be neglected.

The total available power P in the groundwater flux during steady-state flow is hence nearly completely dissipated:

$$P = \rho g \boldsymbol{q} \cdot \nabla H = -D \ (Eq. 7).$$

By inserting Darcy's law into Eq. 7 and recalling that we focus on a two-dimensional domain, we obtain an equation that relates power and dissipation to the squared head gradient (in sense of a scalar product):

$$P = -\rho g K \left[\frac{\partial \mathrm{H}}{\partial \mathrm{x}}\frac{\partial \mathrm{H}}{\partial \mathrm{x}} + \frac{\partial \mathrm{H}}{\partial \mathrm{y}}\frac{\partial \mathrm{H}}{\partial \mathrm{y}}\right] = -D \ (Eq. 8).$$

The physical mechanism that causes dissipation relates to the shear and frictional losses the fluid experiences when passing through the porous medium. As hydraulic conductivity relates to the ratio of intrinsic permeability k (m^2) and viscosity of the fluid η (N sm^{-1}), the inverse of

https://doi.org/10.5194/hess-2021-254
Preprint. Discussion started: 21 May 2021
© Author(s) 2021. CC BY 4.0 License.

Hydrology and Earth System Sciences
Discussions

K is a measure of the flow resistance and related dissipative losses. One would thus expect that the dissipative losses grow with fluid viscosity (declining *K*, increasing resistance) and declining permeability (declining *k*). To better underpin this, we simplify Eq. 8 for steady-state flow through an heterogeneous, one-dimensional system, which means that $\frac{\partial \mathrm{H}}{\partial \mathrm{y}}$=0:

$$P = \rho g(K(x)\mathrm{d}_x H)\mathrm{d}_x H = D(x)\ (Eq.9).$$

where d_x denotes the gradient with respect to *x*. Steady-state flow in one dimension implies a constant flux *q* in the *x* direction, which means that the total spatial variation of d*q* is zero. As *K* is spatially variable, this implies that local spatial variations of conductivity denoted by *d*(*K*(*x*)) must be compensated by opposite spatial variations of the pressure head gradient, $d(\mathrm{d}_x H)$:

$$dq = 0 \rightarrow$$

$$d(-K(x)\mathrm{d}_x H) = 0 \rightarrow$$

$$-d\big(K(x)\big)\,\mathrm{d}_x H\ = K(x)\ d(\mathrm{d}_x H)\ \ Eq.(10)$$

As a consequence, power *P* is not constant (Eq. 7) but instead grows with the magnitude of local spatial variations of the head gradient $d(\nabla_x H)$:

$$dP = \rho g q\ d(\mathrm{d}_x H)\ (Eq.11\ ).$$

Due to Eq. 10 (constant Darcy flux), we can express the spatial variation in the head gradient $d(\mathrm{d}_x H)$ in Eq. 11 as follows:

$$-\mathrm{d}_x H\ d\big(\ln\big(K(x)\big)\big) = d\big(\mathrm{d}_x H\big) \qquad (Eq.12).$$

Combining Eq. 12 with Eq. 11, together with the definition of power in Eq. 9, yields:

$$dP = -P(x)\ d\big(\ln\big(K(x)\big)\big) \rightarrow d(\ln(P(x)\big) = -d(\ln\big(K(x)\big)\ (Eq.13\ ).$$

As a consequence, we expect an anti-proportionality between ln(*P*(*x*)) and ln(*K*(*x*)) for the one-dimensional case. In conclusion, we propose that the necessary power to push the fluid through an heterogeneous medium grows also in the two-dimensional case with the variance of the ln(*K*) field. Local areas of high power coincide with large positive deviations from the overall average head gradient, and these in turn peak across regions of low conductivity. This makes sense, as

https://doi.org/10.5194/hess-2021-254
Preprint. Discussion started: 21 May 2021
© Author(s) 2021. CC BY 4.0 License.

Hydrology and Earth System Sciences
Discussions

dissipation peaks in those areas as flow resistance reach a maximum and the required work to push fluid through these bottlenecks grows as well. This potentially explains the finding of Edery et al. (2014) that the preferential flow paths also pass through areas of low conductivity. We discuss this idea further in section 5.

3.3 Characterizing emergent spatial organization in solute transport using information entropy

We now address the connection between physical entropy and information entropy, and explain how we use the latter to quantify ordered states due to the emergence of preferential flow paths and the associated formation of a concentration gradient transversal to the main flow direction. The Shannon entropy S_H (bit) is defined as the expected value of information (Shannon, 1948). Here we defined S_H using the discrete probability distribution to find particles at a distinct transversal position y at a given x coordinate, as detailed below.

The field of information theory, originally developed within the context of communication engineering, deals with the quantification of information with respect to a concept called "surprise" of an event (Applebaum, 1996). For a discrete random variable Y that can take on several values y_i with associated prior probabilities $p(y_i)$ the surprise or information content of receiving/observing a specific value $Y = y_i$ is defined as:

$$I = -\log_b\big(p(y)\big) \quad \text{(Eq. 14)}$$

where I is the information content, b is the base of the logarithm and $p(y_i)$ the prior probability that Y can be observed in the state y. Due to the use of the logarithm in Eq. 14, information is an additive quantity, similar to physical entropy, energy, and mass. The expected information content associated with the probability distribution of the random variable Y is the Shannon entropy S_H:

$$S_H(Y) = -\sum_{y \in Y} p(y_i)\, log_2\ p(y_i) \quad \text{(Eq. 15)}$$

The definition of the Shannon entropy is equivalent to Gibb's definition of physical entropy in statistical mechanics (Ben-Naim, 2008). The latter is obtained when using the natural logarithm in Eq. 15 and by multiplying the sum with the Boltzmann constant (k_B=1.30640 × 10^{-23} J K^{-1}). Physical entropy describes, in terms of statistical mechanics, the number of microstates that

https://doi.org/10.5194/hess-2021-254
Preprint. Discussion started: 21 May 2021
© Author(s) 2021. CC BY 4.0 License.

Hydrology and Earth System Sciences
Discussions

correspond to the same macro-state at a given internal energy. In the state of maximum entropy where all gradients are depleted, each microstate is equally likely (Kondepudi and Prigogine, 1998). The probability *p* of a single state is in this case, hence, simply the inverse of the number of microstates. This implies a maximum uncertainty about the microstates and corresponds to a minimum order in the system. Jaynes (1957) transferred this fundamental insight into a method of statistical inference, stating *"when making inferences based on incomplete information, the best estimate for the probabilities is the distribution that is consistent with all information, but maximizes uncertainty*". We emphasize that a maximum in information entropy and physical entropy commonly implies a zero gradient either in probability (from the information perspective) or in an intensive state variable such temperature, concentration or pressure (from the thermodynamic perspective).

Its straightforward implementation makes Shannon entropy a flexible means (i) for the optimization of observation networks (Fahle et al., 2015; Nowak et al., 2012), (ii) for the characterization of mixing and dilution of solute plumes (e.g., Woodbury and Ulrych, 1993; Kitanidis, 1994), or (iii) to illuminate how spatial disorder in hydraulic conductivity relates to statistical moments of solute breakthrough curves (Bianchi and Pedretti, 2017). Here we adopt a straightforward use of the Shannon entropy to characterize simulated solute transport, as introduced by Loritz et al. (2018) to characterize redundancy in a distributed hydrological model ensemble. We suggest that the maximum uncertainty corresponds to the case where each flow path through the domain is equally likely, and the probability distribution to find particles in a position in the *y*-direction is, hence, uniform. Deviations from this entropy maximum reflect spatial order due to the concentration of particles in preferred flow paths and the associated persistence of a transversal concentration gradient. This can be analyzed by computing the Shannon entropy of the particle density distributions along *y*, $S_H(x)$, at a fixed position *x* along the main flow direction, using the particle density matrix. A state of maximum entropy implies that the same number of particles has visited each of the 120 grid cells at a given *x* coordinate i.e. $S_H^{max} = log_2\,(120) = 6.9$ bits. A state of perfect spatial organization and zero entropy arises, on the other hand, when all particles move through a single grid cell at a distinct coordinate *x*.

https://doi.org/10.5194/hess-2021-254
Preprint. Discussion started: 21 May 2021
© Author(s) 2021. CC BY 4.0 License.

Hydrology and Earth System Sciences
Discussions

4 Results

In the following, we demonstrate that preferential transport is indeed manifested self-organization and showcase that a stronger self-organization requires indeed more physical work. To this end, we calculated the Shannon entropy of transversal flow paths distribution and relate this to power in fluid flow across the range of the variances in ln(K) as detailed below. For this purpose, we set the dimensionless length and time units to meters and seconds, respectively.

4.1 Preferential flow paths and flow path entropy as function of the variance in ln(K)

Figures 2a-c compare the accumulated particle densities that passed through grid cells in the domain as a function of the variance, σ^2, for a randomly selected realization. The solute transport pathways extend in a largely parallel form and share rather similar particle densities for σ^2=1. However, the number of pathways clearly declines with increasing variance, and they exhibit a stronger meandering and a larger visitation of particles in a smaller transversal number of grids on their downstream course. The Shannon entropy S_H of the flow paths (flow path entropy hereafter) exhibits, in general, and for all three variance cases, a clear decline with increasing downstream transport distance (Figs. 2d-f). This reflects the increasing order in the flow path distribution, corresponding to the emerging and increasing transversal concentration gradients. A comparison of S_H among the variance cases clearly corroborates the visual impression that the number preferential flow paths declines with increasing subscale randomness, while the concentration of solutes therein increases. The analysis of flow path entropy within the entire set of 100 realizations revealed that this behavior is not an artefact of single realization. The flow path entropy average across all realization of a variance case exhibits a steady downstream decline (Fig. 3 a), and the curves are clearly shifted to lower values with increasing variance of ln(K). The boxplots in Fig. 3b characterize the distribution of $S_H(x)$ at the downstream outlet among the realizations. While the spreading and the skewness of the distribution clearly increases with increasing variance in ln(K), we also observe that flow path entropy at the outlet declines clearly and statistically significantly with increasing variance.

https://doi.org/10.5194/hess-2021-254
Preprint. Discussion started: 21 May 2021
© Author(s) 2021. CC BY 4.0 License.

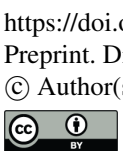

Hydrology and Earth System Sciences
Discussions
Open Access
EGU

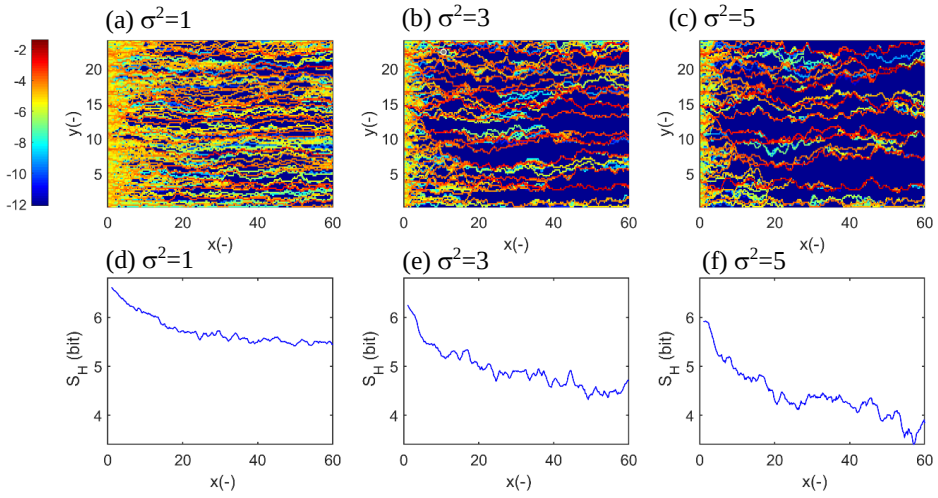

Figure 2: Accumulated, normalized number of particles that passed a distinct point in the domain as function of the variance in ln(K), σ^2, ((a), (b), (c)) and the corresponding Shannon entropy of the transversal concentration, $S_{H,}$ as a function of the main flow direction ((d), (e), (f)).

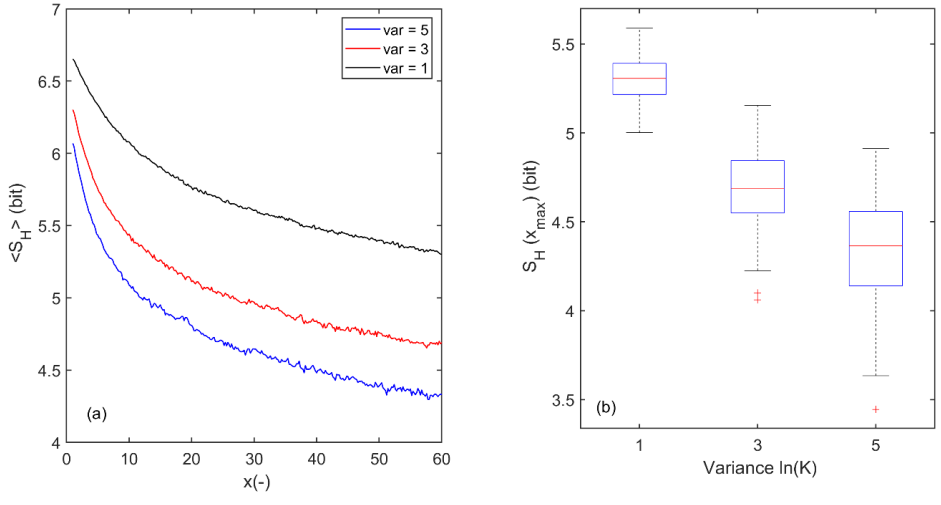

Figure 3: Flow path entropy averaged across all 100 ensemble realizations <S_H> as function of downstream transport distance (a). Boxplot of flow path flow path entropy at the domain outlet for all realizations of the three variance cases (b); note this corresponds to the asymptotic values in (a) at x(-) = 60.

https://doi.org/10.5194/hess-2021-254
Preprint. Discussion started: 21 May 2021
© Author(s) 2021. CC BY 4.0 License.

Hydrology and Earth System Sciences
Discussions
Open Access
EGU

We thus state that a higher variance – and thus randomness – in hydraulic conductivity coincides, for all realizations, with stronger a downstream reduction of the flow path entropy. This corresponds to a macrostate of higher order due to a more efficient self-organization into a state of stronger preferential transport.

4.2 Power in fluid flow as function of the variance in ln(*K*)

Figures 4a-c compare the distribution of power in the fluid flow calculated according to Eq. 7, as a function of the variance of ln(*K*) in the different domains, using a logarithmic scale. For consistency, we used the same ensemble as for Fig. 2. The distributions of power in the fluid generally spread across a wide range of magnitudes and are skewed to the left. However, the distributions clearly shift to larger values and their spread becomes wider when moving to larger variances.

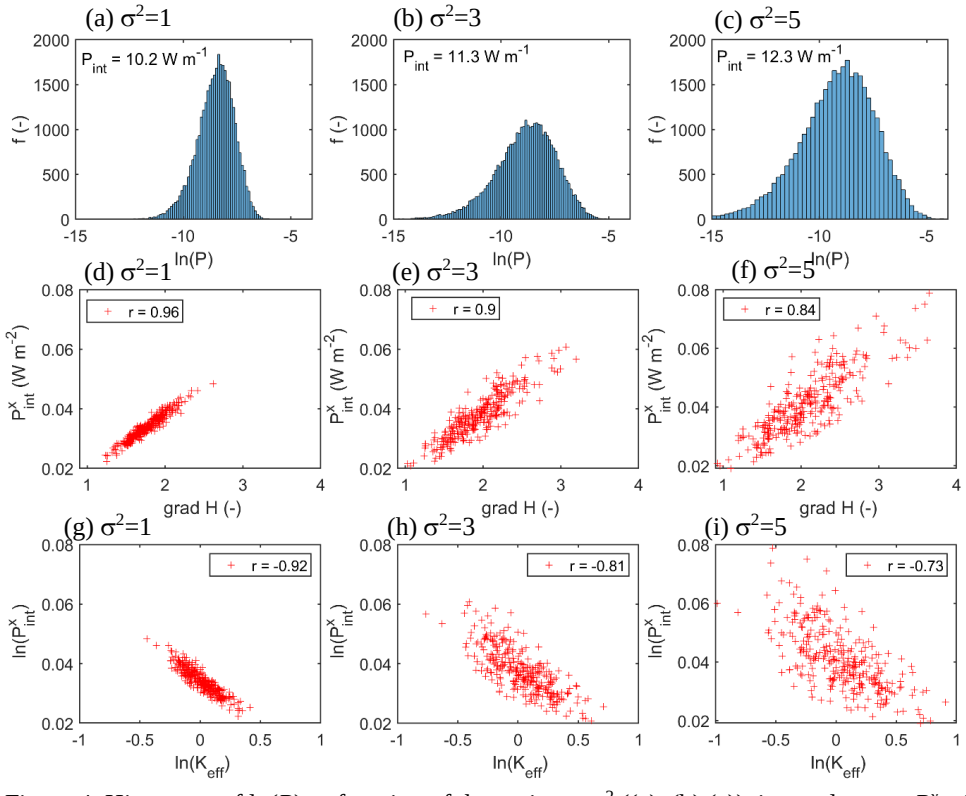

Figure 4: Histogram of ln(*P*) as function of the variance σ^2 ((a), (b) (c)), integral power P^x_{int} in the total downstream water flux, plotted against the laterally averaged head gradient ((d), (e), (f)), and ln(P^x_{int}) as function of the ln of transversally averaged ln(K_{eff}) ((g),(j), (h)).

https://doi.org/10.5194/hess-2021-254
Preprint. Discussion started: 21 May 2021
© Author(s) 2021. CC BY 4.0 License.

Hydrology and Earth System Sciences
Discussions

455 This is underpinned when comparing the integrated power in fluid flow across the entire two-
456 dimensional domain. An increase in variance by two orders of magnitude in the log-normal
457 scale corresponds to an increase in power of 2 W per unit width of the domain. To further
458 illuminate whether the above postulate of a strong linear relation between power and variation
459 in the head gradient exists, we integrated power in fluid flow across the transversal extent of
460 the domain (P^x_{int} hereafter) and plotted it against the laterally averaged head gradient (Fig. 3d-
461 f). In the case of unit variance, this indeed yields a strongly linear relation, with an almost
462 perfectly linear growth of P^x_{int} with the head gradient, as indicated by the correlation coefficient
463 of 0.96. While this the correlation becomes weaker with increasing variance, it remains
464 significant with a correlation coefficient of 0.84 even for the case of $\sigma^2 = 5$. The decline in
465 correlation is plausible as a higher variability in K, in two-dimensional domains, causes stronger
466 transversal flow components and thus a larger deviation from the one-dimensional
467 heterogeneous case for which Eqs. 9 -12 are valid. As expected, the head gradients show also a
468 wider spread with increasing variance (Figs. 3d-f); the same holds true for power in the total
469 downstream fluid flow.

470 To check the inverse-linear relationship between $\ln(P)$ and $\ln(K)$, which was derived for the
471 one-dimensional approximation as well (recall Eqs. 11 - 13), we related $\ln(P^x_{int})$ to the logarithm
472 of laterally averaged conductivity $\ln(K_{eff})$ (Figs. 3g-i). For the unit variance case, we observe
473 an almost perfect linear increase of $\ln(P^x_{int})$ with a decline in $\ln(K_{eff})$, as underpinned by the
474 correlation coefficient of -0.92. This negative correlation declined with increasing variance to
475 a value of -0.81 and -0.72 for $\sigma^2 = 3$ and $\sigma^2 = 5$, respectively. Yet it is still significant, hence the
476 system behaves also in case of the highest variance largely similar to a heterogeneous one-
477 dimensional system. This is because of the confining upper and lower no-flow boundary
478 condition.

479 We thus argue that the power required to maintain the driving head difference and fluid flow in
480 steady state increases with increasing variance of the hydraulic conductivity field. Regions of
481 high power coincide with large positive deviations of the hydraulic head from its mean, and
482 also with “bottlenecks” of low hydraulic conductivity along the preferential pathways.

https://doi.org/10.5194/hess-2021-254
Preprint. Discussion started: 21 May 2021
© Author(s) 2021. CC BY 4.0 License.

Hydrology and Earth System Sciences
Discussions
Open Access
EGU

4.3 Entropy as a function of power and power along solute transport trajectories

Figure 5a shows the Shannon entropy at the downstream outlet $S_H(x_{max})$ as a function of the power in fluid flow integrated over the entire domain P_{int} for all variance cases. The almost perfect linear decline of $S_H(x_{max})$ with P_{int} reveals, in line with the gas laser example given in the introduction, that a larger power input due to a higher pumping rate leads to an higher order in the macroscale preferential transport pattern. We return to this point in section 5.3.

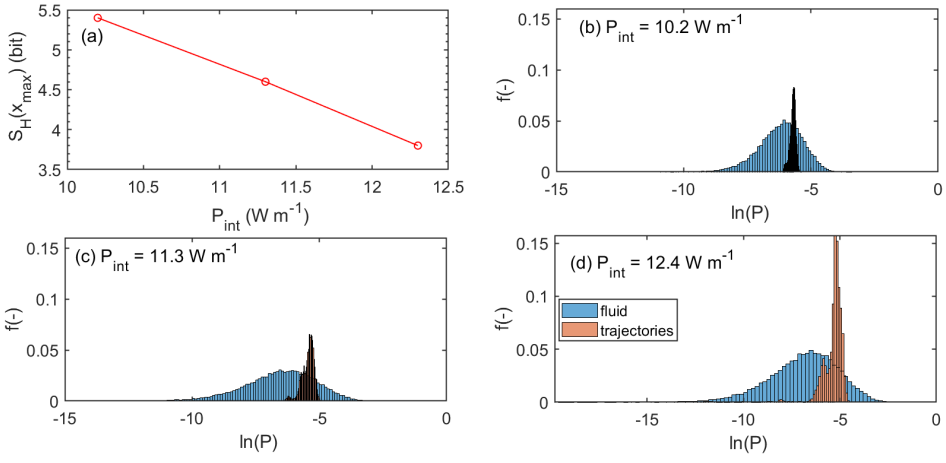

Figure 5: (a) Shannon entropy at the downstream outlet $S_H(x_{max})$ as function of the power in fluid flow integrated over the entire domain P_{int} (a), cumulative distributions of ln(P) in the flow domain (blue) and of ln(P) averaged along the particle trajectories (brown) for the variance cases (b) $\sigma^2 = 1$, (c) $\sigma^2 = 3$, and (d) $\sigma^2 = 5$.

Figures 5b, c, d compare the probability density distributions (pdfs) of ln(P) within the entire flow domain (blue), against the power averaged along the actual particle trajectories (in brown, again on a log scale). While in the case of perfectly mixed flow and transport, both pdfs should be rather similar, they actually are remarkably different. The particles clearly prefer pathways of high power, as the pdfs are clearly shifted towards higher power (Fig. 5 d).

4.4 Space-time asymmetry and entropy export into the breakthough

To switch the observing perspective, we determined the particle breakthrough curves (BTC) for the different variances cases (Fig. 6a) and calculated their Shannon entropy as means of uncertainty and order in the arrival times, using the time step width of 0.1 dimensionless time units as bin width. The width of the breakthrough curves clearly increases with increasing

https://doi.org/10.5194/hess-2021-254
Preprint. Discussion started: 21 May 2021
© Author(s) 2021. CC BY 4.0 License.

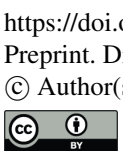

Hydrology and Earth System Sciences
Discussions
Open Access
EGU

504 variance, indicating an earlier breakthrough, a longer tailing and a more even distribution of
505 normalized concentrations in time (Fig. 6 a). This implies that the Shannon entropy in arrival
506 times grows with increasing variance of ln(K) reflecting a larger uncertainty and a declining
507 order in the temporal distribution of travel times. In this context, it is important to recall that
508 entropy cannot be consumed, due to the second law. This that means that the declining flow
509 path entropy needs to be exported from the system.

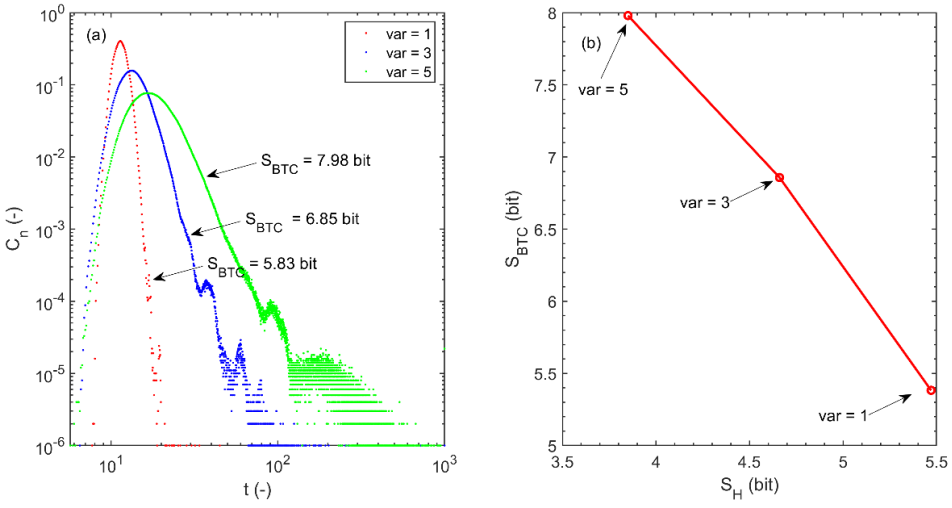

510

511 Figure 6: Breakthrough curves and their Shannon entropies S_{BTC} (a); S_{BTC} plotted against the
512 flow path entropy of the downstream outlet $S_H(x_{max})$, before particles leave the domain, for all
513 variance cases (b).

514 Figure 6b) visualizes this space-time asymmetry in entropies, the growing spatial organization
515 with increasing variance of ln(K) translates due to the associated entropy export into a declining
516 organization in arrival times. Please note that due to the different binning in space and time,
517 changes in S_{BTC} and S_H with changing variance cannot be exactly the same. In fact, also the
518 entropy, which is produced due to energy dissipation, must be exported, but this is much more
519 difficult to quantify. The opposite of the Shannon entropy monotonies corroborate nevertheless
520 that reduced flow path entropy is indeed exported into the BTC. One might hence wonder
521 whether a perfect spatial organization due to preferential transport of the entire solute particles
522 through a single preferential flow path would, in the case of a step input, translate into a BTC

https://doi.org/10.5194/hess-2021-254
Preprint. Discussion started: 21 May 2021
© Author(s) 2021. CC BY 4.0 License.


of maximum entropy/disorder, i.e. rectangular BTC (and vice versa). We return to this issue in sections 5.1 and 6.

5 Discussion

5.1 An energy and entropy centered framework to characterize and explain preferential flow

This study proposes an alternative framework to quantify and explain the enigmatic emergence of preferential flow and transport in heterogeneous saturated porous media, using concepts from thermodynamics and information theory. We examined simulations of two-dimensional fluid flow and solute transport based on the methods of Edery et al. (2014), and characterized the discrete probability distribution associated with finding solute particles crossing a distinct transversal position in a plane normal to the direction of the mean flow by means of the Shannon entropy. In general, we found a declining entropy with increasing downstream transport distance, reflecting a growing downstream self-organization due to the increasing concentration of particles in preferential flow paths. Strikingly, preferential flow patterns with lower entropies emerged when analyzing simulations in media with larger variances in hydraulic conductivity. This implies that macro-states of higher order established, despite the higher subscale randomness of ln (K). The key to explain this almost paradoxical behavior is the finding that the required power to maintain the driving head difference, in steady-state flow, grows with the variance of the hydraulic conductivity field. Due to this larger energy input, the fluid and solutes may perform more work to increase the order in the flow path distribution, through steepening transversal concentration gradients as reflected in lower entropies.

Notwithstanding these findings, we of course recognize that the concepts of entropy, free energy and work are, per se, not new in hydrology. We thus place our findings in context relative to related studies, in the sections below.

5.2 Measuring irreversibility and macroscale organization using the Shannon entropy

Here we show that the Shannon entropy of the transversal distribution of solutes is suited to quantify the downstream emergence of preferential solute movement, as reflected in a declining "flow path entropy". Lower flow path entropies and thus a stronger spatial order in preferential transport are established when solutes are transported through stronger heterogeneous hydraulic

https://doi.org/10.5194/hess-2021-254
Preprint. Discussion started: 21 May 2021
© Author(s) 2021. CC BY 4.0 License.

Hydrology and Earth System Sciences
Discussions

conductivity fields. In this context, we recall that Edery et al. (2014) analyzed breakthrough curves using the continuous time domain random walk framework (Berkowitz et al., 2006). When fitting an inverse power law to the breakthrough curves, the corresponding ß parameter (which is a measure of the degree of anomalous transport, with ß increasing to 2 indicating Fickian transport) increased with increasing variance of ln(K). Here we analyzed the Shannon entropy of the breakthrough curves in time, and contrary to the flow path entropies, they grow with increasing variance of ln(K). This means that higher degrees in spatial order in solute transport that emerges at larger variances in ln(K), expressed by lower flow path entropies, translate into a higher entropy and thus a higher disorder and thus uncertainty in arrival times. This is reflected by an earlier first breakthrough, a retarded appearance of the peak concentration, and a longer tailing in the breakthrough curves and higher similarity of the BTC to a uniform, rectangular pulse. This finding coincides well with the illustrative case that Bianchi and Pedretti (2017) used to compare solute breakthrough through ordered and disordered alluvial aquifers.

This space-time asymmetry in entropy and organization can, however, only be explained using the physical perspective of entropy and the second law. The emergence of spatially organized preferential transport and the related decline in flow path entropy essentially requires an export of the entropy from the system into the BTC. We thus conclude that the ß parameter of the CTRW framework, is also two-fold measure for spatial organization of solute transport through the system and temporal organization in arrival times and their asymmetry.

5.3 Preferred flow and transport pathways as maximum power structures?

The idea that preferential flow coincides with a larger power in fluid flow has been discussed widely in hydrology. Howard (1971, cited in Howard, 1990) proposed that angles of river junctions are arranged in such way that they minimize stream power; later he postulated that the topology of river networks reflects an energetic optimum, formulated as a minimum in total energy dissipation in the network (Howard, 1990). This work inspired Rinaldo et al. (1996) to propose the concept of minimum energy expenditure as an enslavement principle for the self-organized development of river networks. Hergarten et al. (2014) transferred this concept to groundwater systems. They derived preferential flow paths that minimize the total energy dissipation at a given recharge, under the constraint of a given total porosity and showed that these setups allowed predictions of spring discharge at several locations. Minimum energy

https://doi.org/10.5194/hess-2021-254
Preprint. Discussion started: 21 May 2021
© Author(s) 2021. CC BY 4.0 License.

Hydrology and Earth System Sciences
Discussions

expenditure in the river network implies that power therein is maximized. In this light, Kleidon et al. (2013) showed that directed structural growth in the topology of connected river networks can be explained through a maximization of kinetic energy transfer to transported suspended sediments.

Our findings are in line with but step beyond these studies, which commonly refer to preferential flow in connected, highly conductive networks. Here we find that solute particles prefer to move through pathways of very high power, even when they are not connected by a continuous set of cells of relatively high hydraulic conductivity. On the contrary, these pathways incorporate regions of low hydraulic conductivity. This finding reflects the squared dependence of power on the spatial head gradient, which in turn becomes largest in regions of low hydraulic conductivity. We stress that this result, and our finding that a larger power input (due to a higher pumping rate) leads to a higher order in the macroscale preferential transport pattern, is a consequence of the imposed boundary condition. A steady-state head difference implies a positive energetic feedback: in a real-world experiment, the pump provides this feedback, as otherwise the gradient is depleted by the flowing fluid. Although such a positive feedback is straightforwardly established in a numerical model by assigning the desired constant head difference, it is important that this choice implies that such a positive feedback exists. Due to this virtual energy input, the fluid and solutes may perform the necessary work to rapidly pass through low conductivity bottlenecks and form an ordered preferential flow pattern at the macroscale. The higher necessary pumping rate and energy input into the domains with a larger variance in K explain, furthermore, why preferential flow patterns of higher order emerge with growing subscale randomness.

6 Conclusions and outlook

Based on the presented findings, we conclude that the combined use of free energy and entropy holds the key to characterize and quantify the self-organized emergence of preferential flow phenomena and to explain the underlying cause of their emergence. Information entropy is an excellent, straightforward concept to diagnose self-organization in space and time: Here, the formation of preferential transport is reflected in the downstream decline in the entropy of the transversal flow path distribution and that this decline becomes stronger with increasing variance of hydraulic conductivity. The concepts of free energy and physical entropy, however,

https://doi.org/10.5194/hess-2021-254
Preprint. Discussion started: 21 May 2021
© Author(s) 2021. CC BY 4.0 License.

Hydrology and Earth System Sciences
Discussions

provide the underlying cause: steepening of transversal concentration gradients requires work, the formation of even steeper gradients and lower flow path entropies needs even more work and thus a higher free energy input into the open system. The higher necessary pumping rate and energy input into the domains is the reason, why spatial organization in preferential solute movement increased with growing subscale randomness of hydraulic conductivity. This is behavior is very much in line with what we discussed for the gas laser in the introduction.

Entropy can, however, due to the second law not be consumed, and the declining flow path entropy is in fact be exported from the system into the breakthrough curve. Shannon entropy allows again for the straightforward diagnosis, while physical entropy provides the reason for this space-time asymmetry in entropy, organization and uncertainty. Transport of all solute particles through a single preferential flow paths implied a maximum spatial organization and maximum/knowledge certainty about the transversal spreading of solute. However, this would, due to the entropy export, into a maximum disorder of and thus uncertainty about the arrival times, as the BTC would correspond to rectangular pulse of uniform concentration. Advective diffusive transport through a homogeneous flow field implied, in case of a spatially homogeneous step input, maximum uncertainty about transversal position of solute molecules, while the BTC would be perfectly certain and providing minimum uncertainty about arrival times. This space-time asymmetry in entropy implies that perfect organization and certainty about both flow paths and travel times can never simultaneously occur. This required consummation of entropy and thus violation of the second law of thermodynamics. However, we wonder whether effective predictions of the entropies in the BTC and the flow path distributions based on the knowledge driving head differences and the variance and correlation lengths of hydraulic conductivity might be achievable in the future. This will of course not tell us where solutes move and when they breakthrough, but predict the related uncertainty as an important constraint of transversal distribution of transport pathways and travel times.

Acknowledgments

E.Z. gratefully acknowledges intellectual support by the "Catchments as Organized Systems" (CAOS) research unit and funding of the German Research Foundation, DFG, (FOR 1598, ZE 533/11-1, ZE 533/12-1). Y.E. thanks the support of the Israel Science Foundation (grant No. 801/20); B.B. thanks the support of the Israel Science Foundation (grant No. 1008/20) and the

https://doi.org/10.5194/hess-2021-254
Preprint. Discussion started: 21 May 2021
© Author(s) 2021. CC BY 4.0 License.

Crystal Family Foundation. B.B. holds the Sam Zuckerberg Professorial Chair in Hydrology.

The authors acknowledge support by Deutsche Forschungsgemeinschaft and the Open Access Publishing Fund of Karlsruhe Institute of Technology (KIT). The service charges for this open access publication have been covered by a Research Centre of the Helmholtz Association.

References

Ababou, R., D. McLaughlin, L. W. Gelhar, and A. F. B. Tompson: Numerical simulation of three-dimensional saturated flow in randomly heterogeneous porous media, Transp. Porous Media, 4, 549–565, 1989.

Applebaum, D. (1996). Probability and Information (First). Cambridge University Press.

Becker, M.W. and A.M. Shapiro: Tracer transport in fractured crystalline rock: Evidence of nondiffusive breakthrough tailing, Water Resources Research, 36(7), 1677-1686, 2000.

Ben-Naim: A., A Farewell to Entropy. World Scientific. Chapter 1, https://doi.org/10.1142/6469, 2008.

Berkowitz, B., and Zehe, E.: Surface water and groundwater: unifying conceptualization and quantification of the two "water worlds", Hydrology and Earth System Sciences, 24, 1831-1858, 10.5194/hess-24-1831-2020, 2020.

Berkowitz B. and Scher H.: Anomalous transport in correlated velocity fields, Physical Review E. 81, 1, 11128, 2010.

Berkowitz, B., A. Cortis, M. Dentz, and H. Scher: Modeling non-Fickian transport in geological formations as a continuous time random walk, Rev. Geophys., 44, RG2003, doi:10.1029, 2006.

Berkowitz B.: Characterizing flow and transport in fractured geological media: A review, Advances in Water Resources. 25(8-12), 861-884, 2002.

Beven, K., and Germann, P.: Water-Flow In Soil Macropores .2. A Combined Flow Model, Journal Of Soil Science, 32, 15-29, 1981.

Beven, K., and Germann, P.: Macropores And Water-Flow In Soils, Water Resources Research, 18, 1311-1325, 1982.

Bianchi, M., C. Zheng, C. Wilson, G. R. Tick, G. Liu, and S. M. Gorelick: Spatial connectivity in a highly heterogeneous aquifer: From cores to preferential flow paths, Water Resour. Res., 47, W05524, doi:10.1029/2009WR008966.

Bianchi, M., and Pedretti, D.: Geological entropy and solute transport in heterogeneous porous media, Water Resources Research, 53, 4691-4708, 10.1002/2016wr020195, 2017.

Bolt, G. H., and M. J. Frissel: Thermodynamics of soil moisture, Netherlands journal of agricultural science, 8, 57-78.1960.

Blume, T., E. Zehe, and A. Bronstert: Use of soil moisture dynamics and soil moisture patterns for the investigation of runoff generation processes with special emphasis on preferential flow. Hydrology and Earth System Sciences, 13, 1215 -1233, 2009.

Chiogna, G., and Rolle, M.: Entropy-based critical reaction time for mixing-controlled reactive transport, Water Resources Research, 53, 7488-7498, 10.1002/2017wr020522, 2017.

Cirpka, O.A. and P.K. Kitanidis: Characterization of mixing and dilution in heterogeneous aquifers by means of local temporal moments, Water Resources Research, 36(5), 1221-1236, 2000.

https://doi.org/10.5194/hess-2021-254
Preprint. Discussion started: 21 May 2021
© Author(s) 2021. CC BY 4.0 License.

685 Clausius, R.: Über die Art der Bewegung, welche wir Wärme nennen, Annalen der Physik und
686 Chemie 79, p. 353 – 380, 1857.
687 de Dreuzy, J.-R., J. Carrera, M. Dentz, and T. Le Borgne:Time evolution of mixing in
688 heterogeneous porous media, Water Resour. Res., 48, W06511,
689 doi:10.1029/2011WR011360, 2012.
690 Dekker, L. W., and Ritsema, C. J.: Wetting patterns and moisture variability in water repellent
691 Dutch soils, Journal Of Hydrology, 231, 148-164, 2000.
692 Dell'Oca, A., A. Guadagnini, and M. Riva: Interpretation of multi-scale permeability data
693 through an information theory perspective, Hydrology and Earth System Sciences, 24(6),
694 3097-3109, 2020.
695 Domenico, P. A., and F. W. Schwartz: Physical and Chemical Hydrogeology, John Wiley, New
696 York, 1990.
697 Edery, Y., Guadagnini, A., Scher, H., and Berkowitz, B.: Origins of anomalous transport in
698 disordered media: Structural and dynamic controls, Water Resour. Res., 50, 1490-1505,
699 doi:10.1002/2013WR015111, 2014.
700 Fahle, M., Hohenbrink, T. L., Dietrich, O., and Lischeid, G.: Temporal variability of the optimal
701 monitoring setup assessed using information theory, Water Resources Research, 51,
702 7723-7743, 10.1002/2015wr017137, 2015.
703 Fiori, A. and Jankovic, I.: On Preferential Flow, Channeling and Connectivity in Heterogeneous
704 Porous Formations. Math Geosci 44, 133–145. https://doi.org/10.1007/s11004-011-9365-2,
705 2012.
706 Flury, M., Flühler, H., Leuenberger, J., and Jury, W. A.: Susceptibility of soils to preferential
707 flow of water: a field study, Water resources research, 30, 1945-1954, 1994.
708 Groves, C. G., & Howard, A. D.: Early development of karst systems: 1. Preferential flow path
709 enlargement under laminar flow. Water Resources Research, 30(10), 2837–2846.
710 https://doi.org/10.1029/94WR01303, 1994.
711 Gómez-Hernánez, J. J., Sahuquillo, A., and Capilla, J.: Stochastic simulation of transmissivity
712 fields conditional to both transmissivity and piezometric data—I. Theory, Journal of
713 Hydrology, 203, 162-174, https://doi.org/10.1016/S0022-1694(97)00098-X, 1997.
714 Haken, H., *Synergetics: An Introduction; Nonequilibrium Phase Transitions and Self-*
715 *organization in Physics, Chemistry and Biology* 355 p pp., Springer Berlin, 1983.
716 Jackisch, C., L. Angermann, N. Allroggen, M. Sprenger, T. Blume, J. Tronicke, and E. Zehe.
717 Form and function in hillslope hydrology: in situ imaging and characterization of flow-
718 relevant structures, Hydrology and Earth System Sciences, 21(7), 3749-3775, 2017.
719 Jaynes, E. T.: Information Theory and Statistical Mechanics, Phys. Rev. 106, 620, 1957.
720 Guadagnini, A., and S. P. Neuman: Nonlocal and localized analyses of conditional mean steady
721 state flow in bounded, randomly nonuniform domains, 1, theory and computational
722 approach, Water Resour. Res., 35, 2999–3018, 1999.
723 Hergarten, S., G. Winkler, and S. Birk: Transferring the concept of minimum energy dissipation
724 from river networks to subsurface flow patterns, *Hydrology And Earth System Sciences*,
725 *18*(10), 4277-4288, .2014.
726 Howard, A. D.: Theoretical model of optimal drainage networks, Water Resour. Res., 26, 2107-
727 2117, 1990.
728 Klaus, J., and E. Zehe (2011), A novel explicit approach to model bromide and pesticide
729 transport in connected soil structures, Hydrology And Earth System Sciences, 15(7), 2127-
730 2144.
731 Kleidon, A. (2016), Thermodynamic foundations of the Earth system. New York NY:
732 Cambridge University Press.

https://doi.org/10.5194/hess-2021-254
Preprint. Discussion started: 21 May 2021
© Author(s) 2021. CC BY 4.0 License.

Kleidon, A., Zehe, E., Ehret, U., and Scherer, U.: Thermodynamics, maximum power, and the dynamics of preferential river flow structures at the continental scale, Hydrology And Earth System Sciences, 17, 225-251, 10.5194/hess-17-225-2013, 2013.

Kleidon, A., Renner, M., and Porada, P.: Estimates of the climatological land surface energy and water balance derived from maximum convective power, Hydrology And Earth System Sciences, 18, 2201-2218, 10.5194/hess-18-2201-2014, 2014.

Kitanidis, P.K.: The concept of the Dilution Index, Water Resources Research, 30(7), 2011-2026. https://doi.org/10.1029/94WR00762, 1994.

Kondepudi, D., and Prigogine, I.: Modern Thermodynamics: From Heat Engines to Dissipative Structures, John Wiley Chichester, U. K., 1998.

LaBolle, E.M. and G.E. Fogg: Role of molecular diffusion in contaminant migration and recovery in an alluvial aquifer system, Transport in Porous Media 42: 155–179, 2001.

Levy, M., and B. Berkowitz: Measurement and analysis of non-Fickian dispersion in heterogeneous porous media, J. Contam. Hydrol., 64, 203–226, 2003.

Loritz, R., Hrachowitz, M., Neuper, M., and E. Zehe: The role and value of distributed precipitation data in hydrological models, Hydrol. Earth Syst. Sci., 25, 147–167., https://doi.org/10.5194/hess-25-147-2021,2021,

Loritz, R., Gupta, H., Jackisch, C., Westhoff, M., Kleidon, A., Ehret, U., and Zehe, E.: On the dynamic nature of hydrological similarity, Hydrology And Earth System Sciences, 22, 3663-3684, 10.5194/hess-22-3663-2018, 2018.

Loritz, R., Kleidon, A., Jackisch, C., Westhoff, M., Ehret, U., Gupta, H., and Zehe, E.: A topographic index explaining hydrological similarity by accounting for the joint controls of runoff formation, Hydrology And Earth System Sciences, 23, 3807-3821, 10.5194/hess-23-3807-2019, 2019.

Lotka, A. J.: Contribution to the energetics of evolution, Proc Natl Acad Sci USA, 8, 147-151, 1922a.

Lotka, A. J.: Natural selection as a physical principle, Proc Natl Acad Sci USA, 8, 151-154, 1922b.

Malicke, M., Hassler, S. K., Blume, T., Weiler, M., and Zehe, E.: Soil moisture: variable in space but redundant in time, Hydrology and Earth System Sciences, 24, 2633-2653, 10.5194/hess-24-2633-2020, 2020.

Morvillo, M., Bonazzi, A., Rizzo, C.B.:. Improving the computational efficiency of first arrival time uncertainty estimation using a connectivity-based ranking Monte Carlo method. Stoch Environ Res Risk Assess. https://doi.org/10.1007/s00477-020-01943-5, 2021.

Nowak, W., Y. Rubin, and F. P. J. de Barros: A hypothesis-driven approach to optimize field campaigns, *Water Resources Research*, *48*, Nowak, W., Rubin, Y., and de Barros, F. P. J.: A hypothesis-driven approach to optimize field campaigns, Water Resources Research, 48, 10.1029/2011wr011016, 2012.

Paltridge, G. W.: CLIMATE AND THERMODYNAMIC SYSTEMS OF MAXIMUM DISSIPATION, Nature, 279, 630-631, 10.1038/279630a0, 1979.

Rinaldo, A., Maritan, A., Colaiori, F., Flammini, A., and Rigon, R.: Thermodynamics of fractal networks, Physical Review Letters, 76, 3364-3367, 1996.

Ritsema, C. J., Dekker, L. W., Nieber, J. L., and Steenhuis, T. S.: Modeling and field evidence of finger formation and finger recurrence in a water repellent sandy soil, Water Resources Research, 34, 555-567, 1998.

Riva, M., A. Guadagnini, and X. Sanchez-Vila: Effect of sorption heterogeneity on moments of solute residence time in convergent flows, Math. Geosci., 41, 835–853, doi:10.1007/s11004-009-9240-6, 2009.

https://doi.org/10.5194/hess-2021-254
Preprint. Discussion started: 21 May 2021
© Author(s) 2021. CC BY 4.0 License.

Hydrology and Earth System Sciences
Discussions

781 Shannon, C. E.: A Mathematical Theory Of Communication, *Bell System Technical Journal*,
782 *27*(4), 623-656, 1948.
783 Sternagel, A., R. Loritz, W. Wilcke, and E. Zehe: Simulating preferential soil water flow and
784 tracer transport using the Lagrangian Soil Water and Solute Transport Model, Hydrology
785 And Earth System Sciences, 23(10), 4249-4267, 2019.
786 Sternagel, A., R. Loritz, J. Klaus, B. Berkowitz, and E. Zehe: Simulation of reactive solute
787 transport in the critical zone: a Lagrangian model for transient flow and preferential
788 transport, Hydrology and Earth System Sciences, 25(3), 1483-1508,(2021.
789 Schroers, S., Eiff, O., Kleidon, A., Wienhöfer, J., and Zehe, E.: Hortonian Overland Flow,
790 Hillslope Morphology and Stream Power I: Spatial Energy Distributions and Steady-state
791 Power Maxima, Hydrol. Earth Syst. Sci. Discuss. [preprint], https://doi.org/10.5194/hess-
792 2021-79, in review, 2021.
793 Šimůnek, J., Jarvis, N. J., van Genuchten, M. T., and Gärdenäs, A.: Review and Comparison of
794 models for describing non-equilibrium and preferential flow and transport in the vadose
795 zone, Journal of Hydrology, 272, 14-35, 2003.
796 Tietjen, B., E. Zehe, and F. Jeltsch: Simulating plant water availability in dry lands under
797 climate change: A generic model of two soil layers, Water Resources Research, 45.
798 https://doi.org/10.1029/2007WR006589,(2009.
799 Uhlenbrook, S.: Catchment hydrology - a science in which all processes are preferential -
800 Invited commentary, Hydrological Processes, 20, 3581-3585, 10.1002/hyp.6564, 2006.
801 van Schaik, L., J. Palm, J. Klaus, E. Zehe, and B. Schroeder: Linking spatial earthworm
802 distribution to macropore numbers and hydrological effectiveness, Ecohydrology, 7(2), 401-
803 408, 2014.
804 Wienhofer, J., and E. Zehe: Predicting subsurface stormflow response of a forested hillslope -
805 the role of connected flow paths, Hydrology And Earth System Sciences, 18(1), 121-138,
806 2014.
807 Wienhöfer, J., K. Germer, F. Lindenmaier, A. Färber, and E. Zehe: Applied tracers for the
808 observation of subsurface stormflow on the hillslope scale, *Hydrology and Earth System*
809 *Sciences*, *13*(1145-1161), 2009.
810 Willmann, M., J. Carrera and X. Sánchez-Vila: Transport upscaling in heterogeneous aquifers:
811 What physical parameters control memory functions? Water Resources Research, 44,
812 W12437, doi:10.1029/2007WR006531, 2008.
813 Woodbury A.D. and T. J. Ulrych: Minimum relative entropy: Forward probabilistic modeling,
814 Water Resources Research, 29(8), 2847-2860, https://doi.org/10.1029/93WR00923, 1993.
815 Zehe, E., and Fluhler, H.: Preferential transport of isoproturon at a plot scale and a field scale
816 tile-drained site, Journal of Hydrology, 247, 100-115, 2001.
817 Zehe, E., Blume, T., and Bloschl, G.: The principle of 'maximum energy dissipation': a novel
818 thermodynamic perspective on rapid water flow in connected soil structures, Philos.
819 Trans. R. Soc. B-Biol. Sci., 365, 1377-1386, 10.1098/rstb.2009.0308, 2010.
820 Zehe, E., Ehret, U., Blume, T., Kleidon, A., Scherer, U., and Westhoff, M.: A thermodynamic
821 approach to link self-organization, preferential flow and rainfall-runoff behaviour,
822 Hydrology And Earth System Sciences, 17, 4297-4322, 10.5194/hess-17-4297-2013,
823 2013.
824 Zehe, E., Loritz, R., Jackisch, C., Westhoff, M., Kleidon, A., Blume, T., Hassler, S. K., and
825 Savenije, H. H.: Energy states of soil water - a thermodynamic perspective on soil water
826 dynamics and storage-controlled streamflow, Hydrology And Earth System Sciences, 23,
827 971-987, 10.5194/hess-23-971-2019, 2019.
828